White-Light OLEDs Using Liquid Crystal Polymer Networks

Alicia Liedtke, Mary O'Neill,* Anke Wertmöller, Stuart P. Kitney, and Stephen M. Kelly

Department of Physics, University of Hull, Cottingham Road, Hull HU6 7RX, United Kingdom,
Department of Chemistry, University of Hull, Cottingham Road, Hull HU6 7RX, United Kingdom

We have mixed nematic light-emitting liquid crystals and incorporated them as insoluble cross-linked polymer networks in a liquid crystal white-light organic light-emitting diode (LC-WOLED). The light emission is not voltage-dependent and polarized white light emission is also demonstrated. This wet-chemistry approach to WOLEDs is compatible with patterning by photolithography as well as by inkjet printing at room temperature on plastic substrates by roll-to-roll manufacturing.

Introduction

White-light organic light-emitting diodes (WOLEDs) are being intensively developed as backlights for LCDs (combined with active matrix addressing and color filters) as well as for solid-state lighting[1–3] WOLEDs using either small molecules[4–8] or polymers[9–13] have been reported in many different configurations. Small molecules deposited on the device substrate by vacuum sublimation under high vacuum have been used in WOLEDs as pure single components,[4] red, green, and blue chromophores doped in a small molecule host,[5] in multilayer structures[6] and in stacked OLEDs (SOLEDs)[7] as well as cavities and quantum wells.[8] Alternatively WOLEDs have been developed using many kinds of polymer-based materials, such as polyaniline,[9] polymer blends,[10] doped polymers,[11] copolymers,[12] and side-chain polymers.[13] Polymers can be deposited from solution using spincoating, doctor blade techniques, inkjet printing, etc., which are much cheaper deposition processes than vacuum deposition.[14] White light emission has been generated by eximer/exiplex emission from small molecules[15] and polymers.[16] Hybrid inorganic/polymer WOLEDs[17] and white-light emission for assemblies of iridium and europium complexes[18] have also been reported. Mixtures of liquid crystalline oligomers in the glassy state have been used to generate white light and polarized white light by Förster energy transfer in LC-WOLEDs.[19] However, the oliogomer approach to OLEDs suffers from the same disadvantages as polymers, such as interlayer mixing, high glass transition temperature requirement, problems with multilayer formation due to solubility issues.[14]

We now report a new approach to WOLEDs using insoluble electroluminescent liquid crystalline polymer networks. The electroluminescent liquid crystals are deposited from solution, e.g., by spincoating, doctor blade techniques, and inkjet printing, and then stabilized as insoluble cross-linked polymer networks by lithographic processing.[19,20,22–26] This facilitates the fabrication of multilayer WOLEDs as each cross-linked layer is insoluble in organic solvents used to deposit the following layer.[20] In this report, binary mixtures

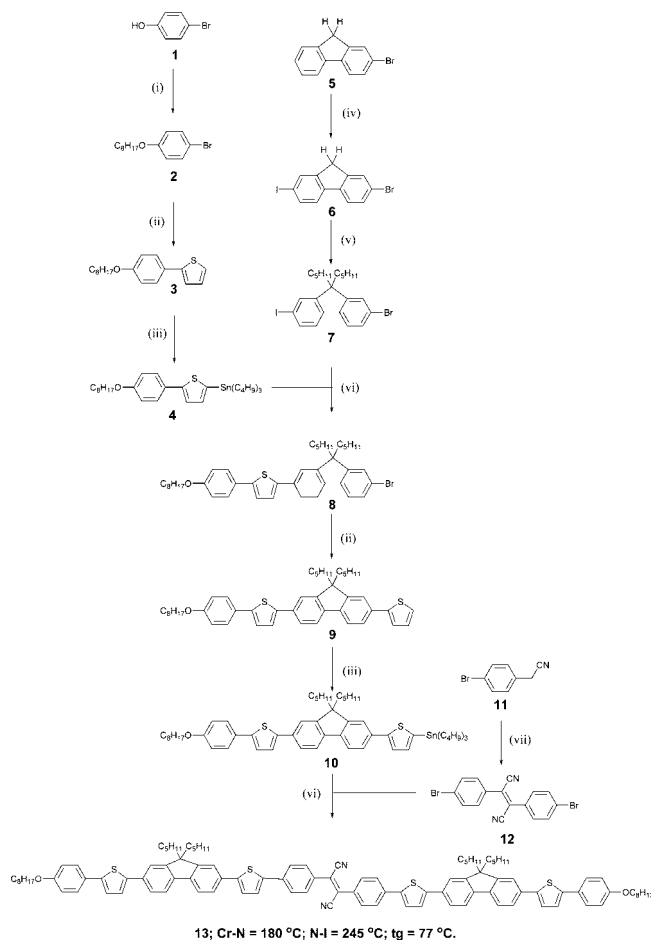* Corresponding author. E-mail: m.oneill@hull.ac.uk (M.O.); s.m.kelly@hull.ac.uk (S.M.K.).

(1) Friend, R. H.; Gymer, R. W.; Holmes, A. B.; Burroughs, J. H.; Marks, R. N.; Taliani, C.; Bradley, D. D. C.; Dos Santos, D. A.; Brèdas, J. L.; Löglund, M.; Salaneck, W. R. *Nature* **1999**, *397*, 121.
(2) Gong, X.; Ma, W.; Ostrowski, J. C.; Bazan, G. C.; Moses, D.; Heeger, A. J. *Adv. Mater.* **2004**, *16*, 615.
(3) D'Andrade, B. W.; Forrest, S. R. *Adv. Mater.* **2004**, *16*, 1585.
(4) Hamada, Y.; Sano, T.; Fujii, H.; Nisio, Y. *Jpn. J. Appl. Phys.* **1996**, *35*, L1339.
(5) (a) D'Andrade, B. W.; Holmes, R. J.; Forrest, S. R. *Adv. Mater.* **2004**, *16*, 624. (b) Ko, B. C. W.; Tao, Y. T. *Appl. Phys. Lett.* **2001**, *79*, 4234.
(6) (a) D'Andrade, B. W.; Thompson, M. E.; Forrest, S. R. *Adv. Mater.* **2002**, *14*, 147. (b) Kim, C. H.; Shinar, J. *Appl. Phys. Lett.* **2002**, *80*, 2201. (c) Strukelj, M.; Jordan, R. H.; Dodabalapur, A. *J. Am. Chem. Soc.* **1996**, *118*, 1213. (d) Kido, J.; Kimura, M.; Nagai, K. *Science* **1995**, *267*, 1332.
(7) (a) Gu, G.; Parthasathy, G.; Burrows, P. E.; Tian, P.; Hill, I. G.; Kahn, A.; Forrest, S. R. *J. Appl. Phys.* **1999**, *86*, 4067. (b) Shen, Z.; Burrows, P. E.; Bulovic, V.; Forrest, S. R.; Thompson, M, E. *Science* **1997**, *276*, 2009.
(8) (a) Liu, S.; Huang, J.; Xie, Z.; Wang, Y.; Chen, B. *Thin Solid Films* **2000**, *363*, 294. (b) Xie, Z. Y.; Huang, J. S.; Li, C. N.; Liu, S. Y.; Wang, Y.; Li, Y. Y. Q.; Shen, J. C. *Appl. Phys. Lett.* **1999**, *74*, 641.
(9) Chen, S.-A.; Chuang, K.-R.; Chao, C.-I.; Lee, H.-T. *Synth. Met.* **1996**, *82*, 207.
(10) (a) Tasch, S.; List, E. J. W.; Erikström, O.; Grauper, W.; Leising, G.; Schlichting, P.; Rohr, U.; Geerts, Y.; Scherf, U.; Müllen, K. *Appl. Phys. Lett.* **1997**, *71*, 2883. (b) Bergren, M.; Inganäs, O.; Gustafsson, G.; Rasmusson, J.; Andersson, M. R.; Hjertberg, T.; Wennerström, O. *Nature* **1994**, *372*, 444. (c) Granstrom, M.; Inganäs, O. *Appl. Phys. Lett.* **1996**, *68*, 147.
(11) (a) Kido, J.; Hongawa, K.; Okuyama, K.; Nagai, K. *Appl. Phys. Lett.* **1994**, *64*, 815. (b) Kido, J.; Shionoya, H.; Nagai, K. *Appl. Phys. Lett.* **1995**, *67*, 2281. (c) Lin, H.-C.; Tsai, C.-M.; Lin, J.-T.; Thomas, K. R. J. *Synth. Met.* **2006**, *156*, 1155.
(12) (a) Baj, S. J.; Wu, C. C.; Dang, T. D.; Arnold, F. E.; Sakaran, B. *Appl. Phys. Lett.* **2004**, *84*, 1656. (b) Lee, Y.-Z.; Chen, X.; Chen, M.-C.; Chen, S.-A. *Appl. Phys. Lett.* **2001**, *79*, 308.
(13) Tokito, S.; Suzuki, M.; Sato, F.; Kamachi, M.; Shirane, K. *Org. Electronics* **2033**, *4*, 105.
(14) Müllen, K., Scherf, U., Eds.; *Organic Light-Emitting Devices: Synthesis, Properties and Applications*; Wiley VCH: New York, 2006.
(15) (a) D'Andrade, B. W.; Brooks, J.; Adamovitch, V.; Thompson, M. E.; Forrest, S. R. *Adv. Mater.* **2002**, *14*, 1032. (b) Feng, J.; Li, F.; Gao, W.; Liu, S. *Appl. Phys. Lett.* **2001**, *78*, 3947.
(16) Chao, C.-I.; Chen, S.-A. *Appl. Phys. Lett.* **1998**, *73*, 426.
(17) (a) Dodabalapur, A.; Rothberg, L. J.; Miller, T. M. **1994**, *65*, 2308. (b) Hide, F.; Kozodoy, P.; Den Baars, S. P.; Heeger, A. J. *Appl. Phys. Lett.* **1997**, *70*, 2664. (c) Zhang, C.; Heeger, A. J. *J. Appl. Phys.* **1998**, *84*, 1579. (d) Tokito, S.; Sakata, J.; Taga, Y. *J. Appl. Phys.* **1995**, *77*, 1985.
(18) Coppo, P.; Duati, M.; Kozhevnikov, V. N.; Hofstraat, J. W.; de Cola, L. *Angew. Chem., Int. Ed.* **2005**, *44*, 1806.
(19) Chen, C. A.; Culligan, S. W.; Geng, Y.; Chen, S. H.; Klubek, K. P.; Vaeth, K. M.; Tang, C. W. *Adv. Mater.* **2004**, *16*, 783.

of electroluminescent (blue and red) liquid crystalline monomers are deposited from solution by spincoating on the substrate surface and then these polymerizable LCs (reactive mesogens, RMs) are photochemically photopolymerised to form highly cross-linked electroluminescent polymer networks. The electroluminescence (EL) spectrum is broad, covers most of the visible spectrum and does not vary with applied voltage as often occurs for mixtures of small molecules and polymers. The use of liquid crystals also allows polarized white-light EL to be demonstrated.[19–26]

The polymerization of light-emitting RMs[20–26] is a promising route to multilayer liquid crystal (LC)-WOLEDs as the self-assembling nature of liquid crystals gives improved carrier mobility[27,28] and polarized emission when uniformly aligned.[19,23,29,30] More importantly, optimal UV exposure without a photoinitiator of a light-emitting, nematic RM gives insoluble and nonmeltable polymer networks with minimal photodegradation of the chromophore and no observable cracking of the polymer layers.[23,31,32] We have recently demonstrated the combination of RMs, OLED technology and standard LCD manufacturing procedures to produce full-color multilayer OLEDs.[20] The patterning of the polarization direction of luminescence is achieved by spatially varying the polarization direction of the ultraviolet light on an appropriate photoalignment layer.[20,23,33,34] Such patterned alignment can be used for 3D displays and holograms. Optimised LC-WOLEDs with polarized white light emission could be used in such 3D displays, holograms and as a backlight for brighter, more energy-efficient LCDs using one polarizer instead of two.

White-light emission is obtained from a new red-emitting LC **13** doped in a range of blue and blue-green emitting LC

Scheme 1[a]

13; Cr-N = 180 °C; N-I = 245 °C; tg = 77 °C.

[a] Reagents and conditions: (i) $C_8H_{17}Br$, K_2CO_3, butanone, reflux; (ii) 2-(tributylstannyl)thiophene, $Pd(PPh_3)_4$, DMF, 90 °C; (iii) (a) *n*-BuLi, THF, −78 °C, (b) $Sn(C_4H_9)_3Cl$; (iv) I_2, H_5IO_6, H_2SO_4, AcOH; (v) $C_5H_{11}Br$, KOH, KI, DMSO; (vi) $Pd(PPh_3)_4$, DMF, 90 °C; (vii) I_2, NaOMe, EtOEt, MeOH, −78 °C.

hosts. The synthesis and liquid crystal transition temperatures of **13** and the blue-green emitting **RM21** are shown in Schemes 1 and 2 respectively. The structure and liquid crystal behavior of the blue-emitting **RM22** and **RM23** are shown in Figure 1. All the compounds exhibit a nematic phase. Compound **13** incorporates a central fumaronitrile moiety as chromophores containing this group in a central position have been shown to be very efficent red electroluminescent materials.[35,36] The compounds **13** and **RM22** and **RM23** are crystalline solids with melting points significantly above room temperature because of their large aspect ratio (length-to-breadth ratio) and large rigid aromatic cores. **RM21** melts at a very low temperature (> −35 °C) because of steric effects attributable to the presence of the large methyl-groups in lateral positions in the molecular core.[24] However, **RM21–RM23** incorporate similar molecular building blocks in the molecular core, i.e., 1,4-disubstituted phenyl, 2,5-disubstituted thiophene and 2,7-disubstituted-9,9-dialkyl-fluorene rings, to ensure a high degree of miscibility of one of these compounds in binary mixtures with compound **13**, which is composed of the same molecular building blocks
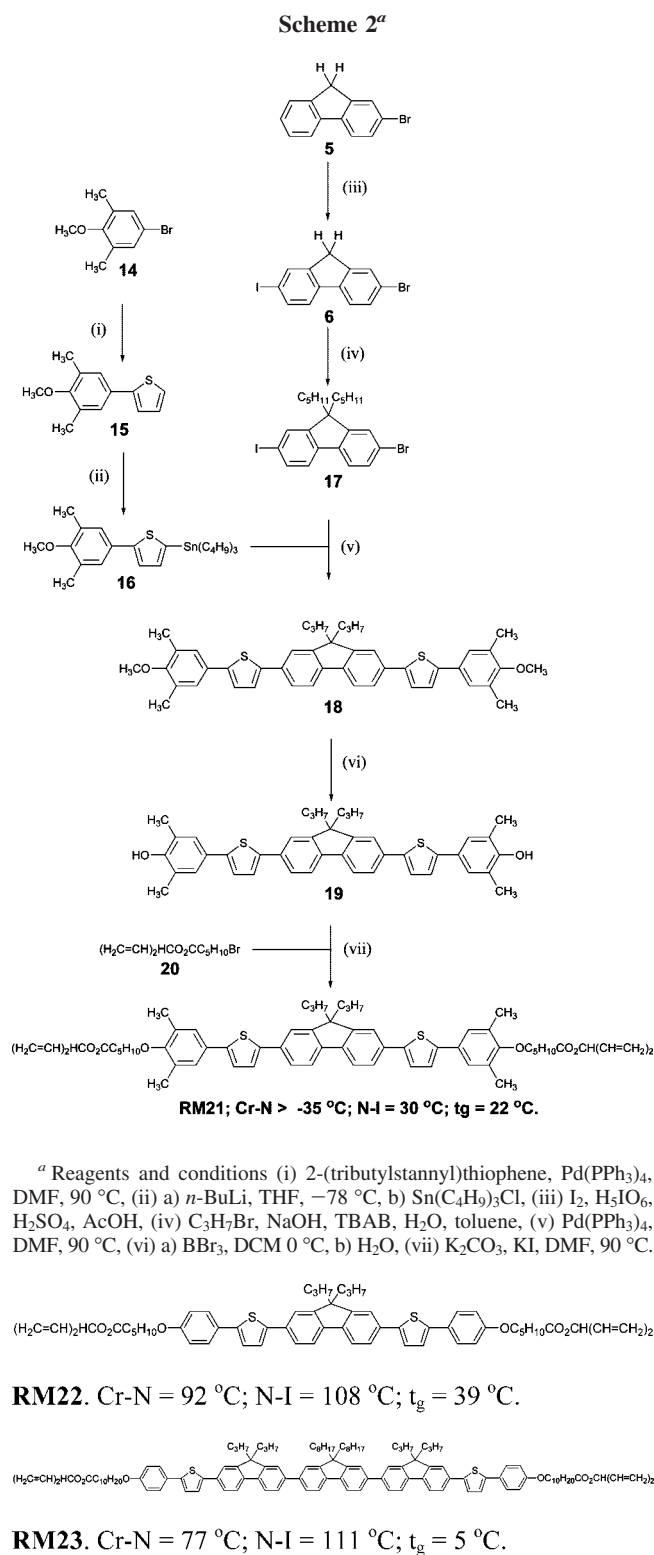
(20) (a) Aldred, M. P.; Contoret, A. E. A.; Farrar, S. R.; Kelly, S. M.; Mathieson, D.; O'Neill, M.; Tsoi, W. C.; Vlachos, P. *Adv. Mater.* **2005**, *17*, 1368. (b) Aldred, M. P.; Eastwood, A. J.; Kitney, S. P.; Richards, G. J.; Vlachos, P.; Kelly, S. M.; O'Neill, M. *Liq. Cryst.* **2005**, *32*, 1251.
(21) Bacher, A.; Erdelen, C. H.; Paulus, W.; Ringsdorf, H.; Schmidt, H. W.; Schuhmacher; P, *Macromolecules* **1999**, *32*, 4551.
(22) Bacher, A.; Bentley, P. G.; Bradley, D. D. C.; Douglas, L. K.; Glarvey, P. A.; Grell, M.; Whitehead, K. S.; Turner, M. L. *J. Mater. Chem.* **1999**, *9*, 2985.
(23) Contoret, A. E. A.; Farrar, S. R.; Jackson, P. O.; May, L.; O'Neill, M.; Nicholls, J. E.; Richards, G. J.; Kelly, S. M. *Adv. Mater.* **2000**, *12*, 971.
(24) Contoret, A. E. A.; Farrar, S. R.; O'Neill, M.; Nicholls, J. E.; Richards, G. J.; Kelly, S. M.; Hall, A. W. *Chem. Mater.* **2002**, *14*, 1477.
(25) Jandke, M.; Hanft, D.; Strohriegl, P.; Whitehead, K.; Grell, M.; Bradley, D. D. C. *Proc. SPIE* **2001**, *4105*, 338.
(26) O'Neill, M.; Kelly, S. M. *Adv. Mater.* **2003**, *15*, 1135.
(27) Christ, T.; Greiner, A.; Sander, R.; Stumpflen, V.; Wendorff, J. H. *Adv. Mater.* **1997**, *9*, 48.
(28) Hassheider, T.; Benning, S. A.; Kitzerow, H. S.; Achard, M. F.; Bock, H. *Angew. Chem., Int. Ed.* **2001**, *40*, 2060.
(29) Geng, Y.; Chen, A. C. A.; Ou, J. J.; Chen, S. H.; Klubek, K.; Vaeth, K. M.; Tang, C. W. *Chem. Mater.* **2003**, *15*, 4352.
(30) Zimmermann, S.; Wendorff, J. H.; Weder, C. *Chem. Mater.* **2002**, *14*, 2218.
(31) Contoret, A. E. A.; Farrar, S. R.; Khan, S. M.; O'Neill, M.; Richards, G. J.; Aldred, M. P.; Kelly, S. M. *J. Appl. Phys.* **2003**, *93*, 1465.
(32) Farrar, S. R.; Contoret, A. E. A.; O'Neill, M.; Nicholls, J. E.; Richards, G. J.; Kelly, S. M. *Phys. Rev. B* **2002**, *66*, 125107.
(33) Sainova, D. S.; Zen, A.; Nothofer, H. H.; Asawapirom, U.; Scherf, U.; Hagen, R.; Bieringer, T.; Kostromine, S.; Neher, D. *Adv. Funct. Mater.* **2002**, *12*, 49.
(34) Jackson, P. O.; O'Neill, M.; Duffy, W. L.; Hindmarsh, P.; Kelly, S. M.; Owen, G. J. *Chem. Mater.* **2001**, *13*, 694.
(35) Yeh, H.-C.; Yeh, S.-J.; Chen, C.-T. *Chem. Commun.* **2003**, 2632.
(36) Huo, L.; Tan, Z.; Han, M.; Li, Y. *Synth. Met.* **2007**, *157*, 690.

White Light OLEDs Using Liquid Crystal Polymer Networks

Chem. Mater., Vol. xxx, No. xx, XXXX **C**

Scheme 2[a]

RM21; Cr-N > **-35 °C; N-I = 30 °C; tg = 22 °C.**

[a] Reagents and conditions (i) 2-(tributylstannyl)thiophene, Pd(PPh₃)₄, DMF, 90 °C, (ii) a) *n*-BuLi, THF, −78 °C, b) Sn(C₄H₉)₃Cl, (iii) I₂, H₅IO₆, H₂SO₄, AcOH, (iv) C₃H₇Br, NaOH, TBAB, H₂O, toluene, (v) Pd(PPh₃)₄, DMF, 90 °C, (vi) a) BBr₃, DCM 0 °C, b) H₂O, (vii) K₂CO₃, KI, DMF, 90 °C.

RM22. Cr-N = 92 °C; N-I = 108 °C; t₉ = 39 °C.

RM23. Cr-N = 77 °C; N-I = 111 °C; t₉ = 5 °C.

Figure 1. Chemical structure and liquid crystal transition temperatures of the reactive mesogens **RM22** and **RM23**.

(see Figure 2). This combination of conjugated aromatic rings, alkyl chains in lateral positions, polymerizable non-conjugated dienes in terminal positions on aliphatic spacer groups has been shown to result in nematic liquid crystals with blue photo- and electroluminescence.[20,23,24] Therefore binary nematic mixtures of components **13** and **RM23** were prepared in order to produce nematic mixtures that could be processed at or near to room temperature. A highly viscous
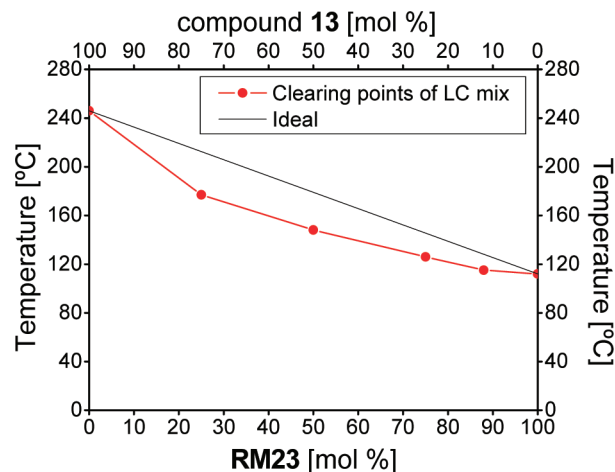

Figure 2. Phase diagram for binary mixtures of **13** and **RM23**. Complete miscibility of the nematic phases of both components is observed for all compositions in the phase diagram using mixtures based on mol %.

vitreous glassy nematic phase is formed at room temperature on cooling from the fluid nematic phase for all of the mixtures prepared. No crystallization on cooling to RT was observed even though compound **13** has a very high melting point (180 °C). This phenomenon is not surprising taking into account the fact that each of the liquid crystals **13** and **RM21–RM23** exhibits a glassy nematic phase at or near room temperature. This behavior is not unusual for liquid crystals of this kind and may, at least in part, be attributable to the very high viscosity of the nematic phase of these materials.[24] The nematic mixtures prepared from these components spontaneously orient on suitable alignment surfaces despite the high viscosity expected for their nematic phases. The glassy state fixes in the desired orientation of the liquid crystals at and above room temperature. Complete miscibility of the components of all of the mixtures was achieved despite the differences in the melting and clearing points of the individual components, e.g., the composition of a series of binary mixtures of the liquid crystals **13** and **RM23** is shown in the phase diagram shown in Figure 2. A normal deviation from ideal behavior (linear plot) for liquid crystalline mixtures is observed and no bulk or microphase phase separation or areas of immiscibility of the mixture components were observed using optical microscopy. A typical Schlieren texture, characteristic of a nematic phase, see Figure 3, is observed between crossed polarisers for the components **13** and **RM21–RM23** as well as for the binary mixtures of the red-emiiting component **13** with the blue emitters **RM21–RM23**. The mixtures are homogeneous and exhibit no phase separation across the mixture phase diagrams.

Experimental Section

General. The structures of intermediates and final products were confirmed by proton (¹H) nuclear magnetic resonance (NMR) spectroscopy (JEOL JMN-GX270 FT nuclear resonance spectrometer), infrared (IR) spectroscopy (Perkin-Elmer 783 infrared spectrophotometer) and mass spectrometry (MS) (Finnegan MAT 1020 automated GC/MS). Reaction progress and product purity was checked using a CHROMPACK CP 9001 capillary gas chromatograph fitted with a 10 m CP-SIL 5CB (0.12 μm, 0.25 mm) capillary
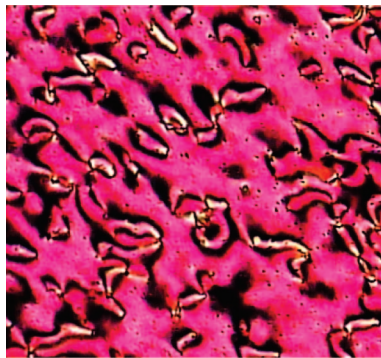
Figure 3. Schlieren texture observed at room temperature between crossed polarisers of the nematic mixture composed of compound **13** (12%) and compound **RM23** (88%).

column. All of the final products were more than 99.5% pure by GLC. Transition temperatures were determined using an Olympus BH-2 polarizing light microscope together with a Mettler FP52 heating stage and a Mettler FP5 temperature control unit. The analysis of transition temperatures and enthalpies was carried out by a Perkin-Elmer DSC7-PC differential scanning calorimeter.[19,20]

1-Bromo-4-(octyloxy)benzene (2). A mixture of 4-bromophenol (**1**) (25.00 g, 0.1445 mol), potassium carbonate (29.96 g, 0.2168 mol), 1-bromooctane (33.49 g, 0.1734 mol), and butanone (400 cm^3) was heated under reflux overnight. The cooled reaction mixture was poured into water (200 cm^3) and the crude product extracted into ethyl acetate (4 × 100 cm^3). The combined organic extracts were washed with brine (200 cm^3) dried (MgSO$_4$), filtered and concentrated under reduced pressure. Purification was carried out via column chromatography [silica gel, hexane] to yield a colorless liquid (28.03 g, 68%). Purity: >98% (GC). ^{1}H NMR (CDCl$_3$): δ_H 0.88 (3H, t), 1.27−1.46 (10H, m), 3.89 (2H, t), 6.75 (2H, d, J = 9 Hz), 7.34 (2H, d, J = 9 Hz). IR ν_{max} (cm^{-1}): 3040, 2960, 2927, 2860, 1608, 1524, 1481, 1290, 1259, 1199, 1133, 1030, 814. MS m/z (EI): 286, 285, 284 (M$^+$), 187, 175, 174 (M 100), 172, 155, 153, 93. Combustion analysis. Expected: C, 58.95; H, 7.42. Obtained: C, 59.09; H, 7.69.

2-[4-(Octyloxy)phenyl]thiophene (3). Tetrakis(triphenylphosphine)palladium(0) (2.03 g, 0.0018 mol) was added to a heated (90 °C) solution of 1-bromo-4-(octyloxy)benzene (**2**) (20.00 g, 0.0701 mol), tributyl(thiophen-2-yl)stannane (26.17 g, 0.0701 mol) and DMF (75 cm^3). The mixture was stirred for 24 h, allowed to cool and poured into a 20% aqueous KF solution (150 cm^3). The crude product was extracted into DCM (3 × 200 cm^3), the combined organic extracts washed with brine (2 × 100 cm^3), dried (MgSO$_4$), filtered, and concentrated under reduced pressure. Purification was carried out via column chromatography [silica gel, DCM:hexane, 1:1] and recrystallized from DCM/EtOH, to yield a white crystalline solid (13.42 g, 66%). Melting point (°C): 69−72. ^{1}H NMR (CDCl$_3$): δ_H 0.89 (3H, t), 1.23−1.36 (10H, m), 1.43−1.48 (2H, m), 1.79 (2H, quint), 3.98 (2H, t), 6.90 (2H, d, J = 8.7 Hz), 7.04 (1H, dd, J = 5, 3.6 Hz), 7.19−7.21 (2H, m), 7.53 (2H, d, J = 8.7 Hz). IR ν_{max} (cm^{-1}): 2923, 1606, 1572, 1531, 1501, 1435, 1393, 1270, 1251, 1169,1086, 1026, 814, 681, 537, 487. MS m/z (EI): 290, 289, 288 (M$^+$), 279, 213, 210, 178, 177, 176 (M 100), 167, 149, 131, 115, 84. Combustion analysis. Expected: C, 74.95; H, 8.39; S, 11.12. Obtained: C, 74.95; H, 8.61; S, 10.97.

Tributyl{5-[4-(octyloxy)phenyl]thiophen-2-yl}stannane (4). A solution of *n*-BuLi in hexane (16.64 cm^3, 2.5 M, 0.0416 mol) was added dropwise to a cooled (−78 °C) solution of 2-(4-(octyloxy)-phenyl)thiophene (**3**) (10.00 g, 0.0347 mol) in THF (150 cm^3). The mixture was stirred for 1 h, maintaining the temperature, followed by the dropwise addition of tributyl tin chloride (13.54 g, 0.0416 mol). The mixture was allowed to warm to RT and stirred overnight.

The crude product was extracted into diethyl ether (2 × 100 cm^3), washed with water (100 cm^3), dried (MgSO$_4$), filtered and concentrated under reduced pressure. No further purification was carried out. Purity: 79% (GC). MS m/z (EI): 577, 576 (M$^+$), 575.

2-Bromo-7-iodofluorene (6). A solution of 2-bromofluorene (**5**) (25.00 g, 0.1000 mol), glacial AcOH (250 cm^3), concentrated sulfuric acid (3 cm^3) and water (20 cm^3) was heated (75 °C), for 10 min. This was followed by the addition of dehydrated periodic acid (4.56 g, 0.0200 mol) and pulverized I$_2$ (10.20 g, 0.0400 mol). After 2 h, the deep purple reaction mixture became yellow in color, indicating completion of reaction, confirmed via GC. Glacial AcOH (100 cm^3) was added and further diluted with sodium metabisulphite solution (2.5 g, 20 cm^3, water). The yellow precipitate was filtered off, washed with MeOH (3 × 250 cm^3), NaOH (5% aq solution, 3 × 250 cm^3), and water (3 × 250 cm^3). The product was then recrystallized from EtOH/DCM, to yield a white crystalline solid (24.45 g, 69%). Melting point (°C):184−186. Purity: >99% (GC). ^{1}H NMR (CDCl$_3$): δ_H 7.48−7.51 (2H, m), 7.60 (1H, d, J = 8.2 Hz), 7.66−7.71 (2H, m), 7.87 (1H, s). IR ν_{max} (cm^{-1}): 1734, 1718, 1635, 1616, 1559, 1539, 1506, 1455, 1436, 1419, 1395, 1050, 1004, 803, 668, 419. MS m/z (EI): 372 (M$^+$), 324, 291, 243, 186, 163, 146, 137, 122, 113, 87, 82 (M 100), 63, 50. Combustion analysis. Expected: C, 42.08; H, 2.17. Obtained: C, 42.38; H, 1.83.

2-Bromo-7-iodo-9,9-dipentylfluorene (7). Powdered potassium hydroxide (6.43 g, 0.1146 mol) was added in small portions to a solution of 2-bromo-7-iodofluorene (**6**) (10.00 g, 0.0270 mol), 1-bromopentane (8.96 g, 0.0593 mol), potassium iodide (0.45 g, 0.0027 mol), and DMSO (200 cm^3) at RT. The deep purple mixture was stirred for 3 h then poured into water (200 cm^3) and the crude product extracted into hexane (4 × 50 cm^3). The combined organic extracts were washed with brine (200 cm^3), dried (MgSO$_4$), filtered and concentrated under reduced pressure. Purification was carried out via column chromatography [silica gel, hexane] and recrystallization from EtOH to yield white needles (9.74 g, 71%). Melting point (°C): 87−89. Purity: >99% (GC). ^{1}H NMR (CDCl$_3$): δ_H 0.66 (6H, t), 0.74−0.81 (4H, m), 1.89 (6H, t), 7.38−7.52 (4H, m), 7.63−7.66 (2H, m). IR ν_{max}/cm^{-1}: 2945, 2920, 2863, 2832, 1890, 1734, 1592, 1570, 1451, 1448,1429, 1399, 1368, 1245, 1208, 1144, 1097, 1050, 1006, 939,870, 809, 750, 741, 669, 667, 494, 423. MS m/z (EI): 511, 510 (M$^+$), 509, 329, 327, 326, 251, 250. Combustion analysis. Expected: C, 54.03; H, 5.52. Obtained: C, 54.30; H, 5.70.

2-(7-Bromo-9,9-dipentylfluoren-2-yl)-5-[4-(octyloxy)phenyl]-thiophene (8). Tetrakis(triphenylphosphine)palladium(0) (0.57 g, 4.9 × 10^{-4} mol) was added to a heated (90 °C) solution of 2-bromo-7-iodo-9,9-dipentylfluorene (**7**) (5.00 g, 0.0098 mol), tributyl{5-[4-(octyloxy)phenyl]thiophen-2-yl}stannane (**4**) (16.94 g, 0.0293 mol), and DMF (100 cm^3). The mixture was stirred overnight, 16 h, allowed to cool, poured into a saturated KF solution (300 cm^3) and the crude product extracted into diethyl ether (3 × 200 cm^3). The combined organic extracts were washed with brine (2 × 250 cm^3), dried (MgSO$_4$), filtered and concentrated under reduced pressure. Purification was carried out via column chromatography [silica gel, DCM:hexane, 1:1] and recrystallized from DCM/EtOH to yield a pale yellow crystalline solid (5.34 g, 81%). Melting point (°C): 128−129. ^{1}H NMR (CDCl$_3$): δ_H 0.58−0.0.72 (11H, m), 0.84−0.89 (22H, M), 1.06 (2H, quint), 1.84 (2H, quint), 1.94−1.98 (4H, m), 6.92 (2H, d, J = 9 Hz), 7.19 (1H, d, J = 3.6 Hz), 7.32 (1H, d, J = 3.7 Hz), 7.52−7.65 (8H, m). IR ν_{max} (cm^{-1}): 2926, 2854, 1605, 1543, 1510, 1460, 1404, 1287, 1249, 1178, 1128, 1042, 998, 879, 828, 795, 726, 662, 498. MS m/z (EI): 673, 672 (M$^+$), 670, 596, 595, 593, 559, 557, 542, 521, 453, 451, 430, 417, 408, 400, 386, 372, 365, 352, 351, 337, 321, 306, 287, 214, 195, 138, 121. Combustion analysis. Expected: C, 73.30; H, 7.65; S, 4.77. Obtained: C, 73.58; H, 7.92; S, 4.50%.

2-[9,9-Dipentyl-7-(thiophen-2-yl)fluoren-2-yl]-5-[4-(octyloxy)-phenyl]thiophene (9). Tetrakis(triphenylphosphine)palladium(0) (0.23 g, 1.95 × 10^{-4} mol) was added to a heated (90 °C) solution of 2-(7-bromo-9,9-dipentylfluoren-2-yl)-5-[4-(octyloxy)phenyl]-thiophene (**8**) (2.60 g, 0.0039 mol), tributyl(thiophen-2-yl)stannane (1.59 g, 0.0043 mol) and DMF (20 cm^3). The mixture was stirred overnight, 16 h, allowed to cool, poured into a saturated KF solution (300 cm^3) and the crude product extracted into diethyl ether (3 × 200 cm^3). The combined organic extracts were washed with brine (2 × 250 cm^3), dried (MgSO$_4$), filtered and concentrated under reduced pressure. Purification was carried out via column chromatography [silica gel, DCM:hexane, 2:1] and recrystallization from DCM/EtOH to yield a yellow crystalline solid (2.30 g, 88%). Melting point (°C): 138−140. ^{1}H NMR (CDCl$_3$): δ_H 0.71 (3H, t), 0.90 (6H, t), 1.04−1.11 (12H, m), 1.27−1.33 (10H, M), 1.81 (2H, quint), 2.00−2.04 (4H, m), 4.00 (2H, t), 6.93 (2H, d, J = 8.7 Hz), 7.11 (1H, dd, J = 5, 3.7 Hz), 7.21 (1H, d, J = 3.6 Hz), 7.30 (1H, d, J = 5, 1.1 Hz), 7.34 (1H, d, J = 4 Hz), 7.38 (1 Hz, dd, J = 3.6, 1.1 Hz), 7.56−7.62 (6H, m), 7.68 (2H, d, J = 7.9 Hz). IR ν_{max} (cm^{-1}): 2890, 2728, 1634, 1510, 1474, 1391, 1298, 1136, 1101, 1044,1021, 999, 850, 757, 664, 465. MS m/z (EI): 676, 675, 674 (M$^+$, M100), 603, 562, 561, 435, 434, 433, 421, 281, 211, 112.

Tributyl[5-(7-{5-[4-(octyloxy)phenyl]thiophen-2-yl}−9,9-di-pentylfluoren-2-yl)thiophen-2-yl]stannane (10). A solution of n-BuLi in hexane (1.35 cm^3, 2.5M, 0.0034 mol) was added dropwise to a cooled (−78 °C) solution of 2-[9,9-dipentyl-7-(thiophen-2-yl)fluoren-2-yl]-5-(4-(octyloxy)phenyl)thiophene (**9**) (2.25 g, 0.0033 mol) in THF (150 cm^3). The mixture was stirred for 1 h, maintaining the temperature, followed by the dropwise addition of tributyl tin chloride (1.19 g, 0.0037 mol). The mixture was allowed to warm to RT and stirred overnight. The crude product was extracted into diethyl ether (2 × 100 cm^3), washed with water (100 cm^3), dried (MgSO$_4$), filtered and concentrated under reduced pressure. No further purification was carried out. MS m/z (MALDI): 964 (M$^+$), 963, 962, 950, 948, 946, 924, 922, 916, 914, 908, 906, 740 (M 100), 675.

2,3-bis(4-Bromophenyl)fumaronitrile (12). A cooled (−78 °C) solution of sodium methoxide (5.79 g, 0.1070 mol), in methanol (40 cm^3) was added dropwise over 30 min to a cooled (−78 °C) solution of iodine (12.95 g, 0.0510 mol), 4-bromophenylacetonitrile (**11**) (10.00 g, 0.0510 mol) and diethyl ether (200 cm^3). The mixture was allowed to warm to 0 °C and stirred for 4 h maintaining the temperature at 0 °C. The mixture was acidified by the addition of HCl(aq) (3%, v/v, 150 cm^3) and the resulting precipitate filtered on a sinter. The crude product was washed on the sinter with water (3 × 200 cm^3), Na$_2$S$_2$O$_5$(aq) (5%, v/v, 3 × 200 cm^3), water (4 × 300 cm^3), and EtOH (2 × 100 cm^3). Purification was carried out by recrystallization from EtOH to yield (8.79 g, 89%) of a pale yellow crystalline solid. Purity: >99% (GC). Melting point (°C): 214−215. ^{1}H NMR (CDCl$_3$): δ_H 7.70 (8H, d, J = 2 Hz). IR ν_{max} (cm^{-1}): 2883, 2538, 2479, 2391, 2234, 2097, 2038, 1960, 1882, 1798, 1671, 1636, 1582, 1440, 1396, 1303, 1249, 1165, 1121, 999, 920, 856, 817, 665. MS m/z (EI): 390, 389, 388 (M$^+$), 387, 308, 307, 230, 229, 228 (M 100), 201, 200, 175, 114. Combustion analysis. Expected: C, 49.52; H, 2.08; N, 7.22. Obtained: C, 50.22; H, 1.85; N, 7.11.

2,3-Bis{4-[5-(7-{5-[4-(octyloxy)phenyl]thiophen-2-yl}-9,9-di-pentylfluoren-2-yl)thiophen-2-yl]phenyl}fumaronitrile (13). Tetrakis(triphenylphosphine)palladium(0) (0.02 g, 1.73 × 10^{-5} mol) was added to a heated (90 °C) solution of tributyl[5-(7-{5-[4-(octyloxy)phenyl]thiophen-2-yl−9,9-dipentylfluoren-2-yl)thiophen-2-yl]stannane (**10**) (2.45 g, 0.0026 mol) 2,3-bis(4-bromophenyl)-fumaronitrile (**12**) (0.20 g, 0.0005 mol) and DMF (30 cm^3). The mixture was stirred overnight, allowed to cool, and poured into a

saturated KF solution (100 cm^3); the crude product extracted into DCM (3 × 200 cm^3). The combined organic extracts were washed with brine (2 × 100 cm^3), dried (MgSO$_4$), filtered, and concentrated under reduced pressure. Purification was carried out via column chromatography [silica gel, DCM:hexane, 4:1] and recrystallization from DCM/EtOH to yield a red crystalline solid (0.38 g, 81%). Transition temp. T_g (°C): 77, Cr; 180, N; 245, I. ^{1}H NMR (CDCl$_3$): δ_H 0.70 (12H, t), 0.88 (6H, t), 1.05−1.08 (12H, m), 1.24−1.35 (14H, m), 1.79 (4H, quint), 2.00−2.05 (8H, m), 4.00 (4H, t), 6.90−6.98 (6H, m), 7.38−7.42 (2H, m), 7.46−7.70 (20H, m), 7.80 (4H, d, J = 9 Hz), 7.92 (4H, d, J = 8.6 Hz). IR ν_{max} (cm^{-1}): 2924, 2853, 1601, 1542, 1509, 1469, 1449, 1280, 1248, 1176, 1027, 883, 829, 797. MS m/z (MALDI):1577, 1576 (M$^+$), 1575, 1574, 816. Combustion analysis. Expected: C, 80.77; H, 7.29; N, 1.78; S, 8.14. Obtained: C, 80.66; H, 7.58; N, 1.91; S, 7.96%.

2-(4-Methoxy-3,5-dimethylphenyl)thiophene (15). Tetrakis-(triphenylphosphine)palladium(0) (2.67 g, 0.0023 mol) was added to a heated (90 °C) solution of 5-bromo-2-methoxy-1,3-dimethyl-benzene (**14**) (10.00 g, 0.0465 mol), tributyl(thiophen-2-yl)stannane (19.09 g, 0.0511 mol) and DMF (100 cm^3). The mixture was stirred overnight, 16 h, allowed to cool, and poured into water (200 cm^3); the crude product extracted into diethyl ether (3 × 200 cm^3). The combined organic extracts were washed with brine (200 cm^3), dried (MgSO$_4$), filtered, and concentrated under reduced pressure. Purification was carried out via column chromatography [silica gel, DCM:hexane, 1:1] to yield a colorless liquid (7.14 g, 70%), which solidified to form a waxy solid over a number of days. Melting point (°C): 44−45. Purity: >98% (GC). ^{1}H NMR (CDCl$_3$): δ_H 2.38 (6H, s), 3.79 (3H, s), 7.10 (1H, dd, J = 4.7, 3.9 Hz), 7.27 (2H, dd, J = 2.5, 1.4 Hz), 7.33 (2H, s). IR ν_{max} (cm^{-1}): 2944, 1479, 1280, 1210, 1006, 890, 876, 740, 510. MS m/z (EI): 220, 219, 218 (M$^+$, M 100), 205, 204, 203, 187, 175, 160, 142, 141, 115, 109, 91, 86.

Tributyl[5-(3,5-dimethyl-4-methoxyphenyl)thiophen-2-yl]stan-nane (16). A solution of n-BuLi in hexane (6.93 cm^3, 2.5M, 0.0173 mol) was added dropwise to a cooled (−78 °C) solution of 2-(4-methoxy-3,5-dimethylphenyl)thiophene (**15**) (3.15 g, 0.0144 mol) in THF (30 cm^3). The mixture was stirred for 1 h, maintaining the temperature, followed by the dropwise addition of tributyl tin chloride (6.57 g, 0.0202 mol). The mixture was allowed to warm to RT and stirred overnight. The crude product was extracted into diethyl ether (2 × 100 cm^3), the combined organic extracts were washed with water (100 cm^3), dried (MgSO$_4$), filtered, and concentrated under reduced pressure. No further purification was carried out. Purity = 73% (GC). MS m/z (EI): 508 (M$^+$), 507, 506, 505, 452, 451, 449, 448, 395, 393, 392, 339, 337, 336, 335, 334, 274, 231, 203, 187, 186, 172, 169, 153, 141, 115.

2-Bromo-7-iodo-9,9-dipropylfluorene (17). A mixture of NaOH (65.00 g), water (130 cm^3), 2-bromo-7-iodofluorene (**6**) (20.00 g, 0.0540 mol), 1-bromopropane (19.94 g, 0.1620 mol), toluene (130 cm^3), and TBAB (0.80 g) was heated under reflux with vigorous stirring overnight, checking completion via TLC. The reaction was allowed to cool and the product extracted into diethyl ether (3 × 250 cm^3). The combined ethereal layers were washed with HCl (10%, 500 cm^3), which produced a color change, green to yellow, and water (3 × 250 cm^3), and then dried (MgSO$_4$), filtered, and concentrated under reduced pressure. Purification was carried out via column chromatography [silica gel, hexane] and recrystallized from EtOH to yield a pale yellow waxy solid (12.05 g, 49%). Melting point /°C: 137−139. Purity: >98% (GC). ^{1}H NMR (CDCl$_3$) δ_H: 0.66 (6H, t), 0.74−0.81 (4H, m), 1.89 (6H, t), 7.38−7.52 (4H, m), 7.63−7.66 (2H, m). IR ν_{max}/cm^{-1}: 2946, 2925, 2866, 2839, 1884, 1734, 1593, 1569, 1454, 1445, 1413, 1394, 1377, 1270, 1239, 1131, 1108, 1050, 1003, 930, 874, 809, 754, 742, 668, 659, 494, 424. MS m/z (EI): 456, 455 (M$^+$), 454 (M 100), 453, 423, 397,

330, 329, 327, 326,251, 250. Combustion analysis. Expected: C, 50.14; H, 4.43. Obtained: C, 50.29; H, 4.42.

bis-2,7-[5-(3,5-Dimethyl-4-methoxyphenyl)thiophen-2-yl]-9,9-dipropylfluorene (18). Tetrakis(triphenylphosphine)palladium(0) (0.28 g, 2.46×10^{-4} mol) was added to a heated (90 °C) solution of 2-bromo-7-iodo-9,9-dipropylfluorene (**17**) (1.12 g, 0.0025 mol), tributyl(5-(4-methoxy-3,5-dimethylphenyl)thiophen-2-yl)stannane (**16**) (5.00 g, 0.0098 mol) and DMF (40 cm³). The mixture was stirred overnight, 16 h, allowed to cool, poured into water (300 cm³) and the crude product extracted into diethyl ether (3 × 200 cm³). The combined organic extracts were washed with brine (2 × 250 cm³), dried (MgSO₄), filtered, and concentrated under reduced pressure. Purification was carried out via column chromatography [silica gel, DCM:hexane, 2:1] and recrystallization from DCM/EtOH to yield a pale yellow crystalline solid (1.43 g, 85%). Transition temp. (°C): Tg 88 Cr 159 N (111) I. ¹H NMR (CDCl₃): δ_H 0.68−0.76 (4H, m), 0.92 (6H, t), 2.02 (4H, t), 2.33 (12H, s), 3.75 (6H, s), 7.23 (2H, d, J = 3.9 Hz), 7.32 (4H, s), 7.35 (2H, d, J = 3.9 Hz), 7.58−7.63 (4H, m), 7.68 (2H, d, J = 7.9 Hz). IR ν_{max} (cm⁻¹): 2925, 1472, 1230, 1180, 1065, 1013, 834, 796, 490. MS m/z (EI): 684, 683, 682 (M⁺), 435, 434, 420, 419, 405, 404, 331, 312, 311, 259, 258, 257, 138, 122, 121, 93, 92. Combustion analysis. Expected: C, 78.86; H, 6.46; S, 9.79. Obtained: C, 78.88; H, 6.32; S, 10.26.

Bis-2,7-[5-(3,5-dimethyl-4-hydroxyphenyl)thiophen-2-yl]-9,9-dipropylfluorene (19). Boron tribromide (2.05 g, 0.0082 mol) was added dropwise to a cooled (0 °C) solution of bis-2,7-[5-(3,5-dimethyl-4-methoxyphenyl)thiophen-2-yl]-9,9-dipropylfluorene (**18**) (1.40 g, 0.0021 mol) in DCM (10 cm³). The reaction mixture was allowed to warm to RT and stirred overnight, poured into ice (300 cm³) and stirred for 1 h. The organic layer was separated and the aqueous layer washed with DCM (3 × 200 cm³); the combined organic layers were dried (MgSO₄), filtered, and concentrated under reduced pressure. Purification was carried out via column chromatography [silica gel, hexane:ethyl acetate, 2:1] to yield a pale yellow crystalline solid (1.08 g, 81%). Melting point /°C: 233. ¹H NMR (CDCl₃): δ_H 0.70−0.73 (4H, m), 0.88 (6H, t), 2.01−2.04 (4H, m), 2.32 (12H, s), 4.70 (2H, s), 7.18 (2H, d, J = 3.9 Hz), 7.30 (4H, s), 7.34 (2H, d, J = 3.9 Hz), 7.60−7.62 (4H, m), 7.67 (2H, d, J = 8 Hz). IR ν_{max} (cm⁻¹): 3432, 2952, 1471, 1239, 1195, 1165, 1067, 872, 798. MS m/z (EI): 656, 655, 654 (M⁺, M 100).

Penta-1,4-dien-3-yl 6-bromohexanoate (20). A solution of 6-bromohexanoyl chloride (25.00 g, 0.1174 mol), in DCM (250 cm³) was carefully added to a solution of 1,4-pentadien-3-ol (10.90 g, 0.1291 mol) and triethylamine (16.30 cm³, 0.1174 mol), in DCM (150 cm³) at 0 °C. The reaction mixture was stirred at 0 °C for 2 h. The white precipitate, [HN⁺(CH₃CH₂)₃Cl⁻], was filtered off and the filtrate concentrated under reduced pressure. Purification was carried out via column chromatography [silica gel, DCM] to yield a colorless oil (23.00 g, 76%). Purity: >99% (GC). ¹H NMR (CDCl₃): δ_H 1.49 (2H, quint), 1.68 (2H, quint), 1.88 (2H, quint), 2.37 (2H, t), 3.41 (2H, t), 5.23 (2H, dt), 5.30 (2H, dt), 5.72 (1H, tt), 5.80−5.88 (2H, m). IR ν_{max} (cm⁻¹): 3100, 3040, 2946, 2886, 1741, 1647, 1465, 1251, 1181, 987, 933, 725. MS m/z (EI): 262, 260, (M⁺), 233, 179, 177, 151, 149, 133, 97, 84, 67 (M).
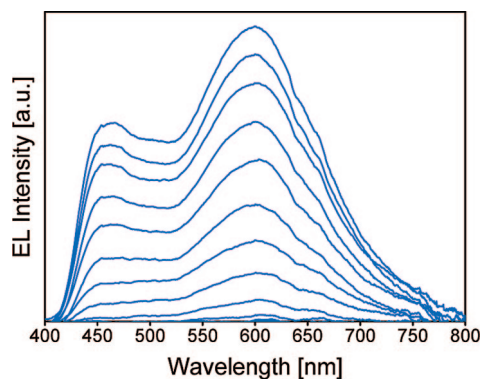
Bis-2,7-(5-{3,5-dimethyl-4-[6-(penta-1,4-dien-3-yl)hexanoyl-oxy]phenyl}thiophen-2-yl)-9,9-dipropylfluorene (21). A mixture of bis-2,7-[5-(3,5-dimethyl-4-hydroxyphenyl)thiophen-2-yl]-9,9-dipropylfluorene (**19**) (0.20 g, 3.05×10^{-4} mol), K₂CO₃ (0.15 g, 0.0011 mol), and DMF (20 cm³) was heated (90 °C) and stirred overnight, 14 h. Penta-1,4-dien-3-yl 6-bromohexanoate (**20**) (0.24 g, 9.16×10^{-4} mol) and BHT (trace amount) were added to the reaction mixture and stirred for a further 24 h. The cooled reaction mixture was poured into water (250 cm³), and the crude product

was extracted into diethyl ether (3 × 150 cm³). The combined organic extracts were washed with water (200 cm³), dried (MgSO₄), filtered and concentrated under reduced pressure. Purification was carried out via column chromatography [silica gel, DCM:hexane, 2:1] to yield a yellow liquid that formed a waxy solid over 2 days (0.19 g, 61%). Transition temp. T_g (°C): 22, Cr; <−35, N; 30, I. ¹H NMR (CDCl₃): δ_H 0.70−0.75 (4H, m), 0.87 (6H, t), 1.54−1.60 (8H, m), 1.76 (4H, quint), 1.85 (4H, quint), 2.02 (4H, t), 2.32 (12H, s), 3.79 (4H, t), 5.23−5.34 (8H, m), 5.73−5.75 (2H, m), 5.81−5.89 (4H, m), 7.23 (2H, d, J = 3.9 Hz), 7.31 (4H, s), 7.34 (2H, d, J = 3.9 Hz), 7.57−7.62 (4H, m), 7.67 (2H, d, J = 7.9 Hz). IR ν_{max} (cm⁻¹): 2954, 2868, 1736, 1600, 1549, 1498, 1478, 1374, 1299, 1242, 1158, 991, 929, 877, 808, 449. MS m/z (MALDI): 1017, 1016, 1015, 1014 (M⁺), 991, 571. Combustion analysis. Expected: C, 76.88; H, 7.35; S, 6.32. Obtained: C, 76.89; H, 7.38; S, 6.54.

Methods. The mesomorphic behavior of compounds **13** and **RM21−RM23** were investigated between crossed polarizers using optical microscopy. The only phase observed was the nematic phase. Nematic droplets are observed on cooling from the isotropic liquid to form the Schlieren texture with two- and four-point brushes characteristic of the nematic phase along with optically extinct homeotropic areas. As the sample is cooled further, the texture often formed more optically extinct homeotropic areas, which indicates that the phase is optically uniaxial. The birefringent and homeotropic areas flashed brightly on mechanical disturbance. This behavior and the simultaneous presence of both the homeotropic and the Schlieren texture confirms that the mesophase observed is indeed a nematic phase.

The values for the liquid crystal transition temperatures of compounds **13** and **RM21−RM23** were confirmed by DSC. Good agreement (≈1−2 °C) with those values determined by optical microscopy were obtained. These values were determined twice on heating and cooling cycles on the same sample. The values obtained on separate samples of the same compounds were reproducible and usually very little thermal degradation was observed even at relatively high temperatures. The baseline of the DSC traces is relatively flat and sharp transition peaks are observed. The melting point (Cr−N and Cr−I) and the clearing point (N−I) are both first order, as expected. A degree of supercooling below the melting point is often observed on the cooling cycle and the compounds **13** and **RM21−RM23** may remain nematic at room temperature for several hours, although their melting points are often much higher than room temperature. This may be attributed, at least in part, to the high viscosity of the nematic phase of these materials and the presence of a glass transition for all of the compounds **13** and **RM21−RM23**.

Device Preparation and Evaluation. OLEDs were fabricated on a glass substrate (25 mm × 45 mm × 1 mm) covered with an ITO transparent anode and a poly(3,4-ethylenedioxythiophene) poly-(styrenesulfonate) aqueous dispersion (PEDOT/PSS BAYTRON P VP AI 4083, H.C. Starck) EL grade layer (thickness 45 nm) deposited by spin-coating. The PSS/PEDOT layer was baked at 50 °C for 5 min and subsequently at 165 °C for 10 min in order to cure the layer and remove volatile components. Thin films of the mixtures of light-emitting materials **13** and **RM21−RM23** were prepared by spin coating from a 0.5−2.0% weight solution in toluene followed by baking at temperatures close to the clearing points of blue-emitting compounds **RM21−RM23**. Some of the films employing compound **RM23** were cross-linked by UV light using a HeCd laser at 325 nm. Fluences of 400 J cm⁻² were required to render the films completely insoluble. A hole-blocking layer (10−15 nm) of tri(phenyl-2-benzimidazolyl)benzene (TPBi) was deposited on top of the cross-linked emission layer by vapor deposition using a vacuum of 1×10^{-6} mbar. Layers of lithium

White Light OLEDs Using Liquid Crystal Polymer Networks

Chem. Mater., Vol. xxx, No. xx, XXXX **G**

Figure 4. Electroluminescence from a cross-linked polymer network formed by photopolymerising a nematic mixture of compounds **13** (12%) and **RM23** (88%) measured at 22 °C for various voltages.
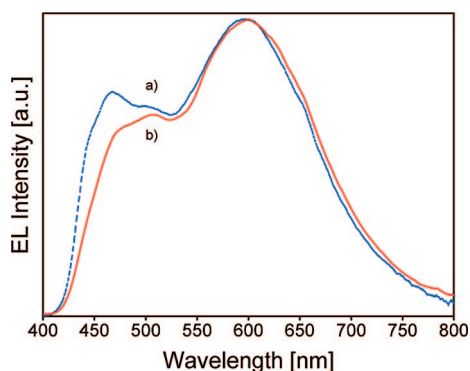
Figure 5. The electroluminescence emission of a) the nonpolymerized nematic mixture **13** (12%) and **RM23** (88%) and b) the EL spectrum of the corresponding cross-linked nematic polymer network formed by photochemically polymerizing this nematic mixture.

Figure 6. CIE diagram for the electroluminescence from three OLEDs: (D1) nematic mixture of **13** and **RM21**; (D2) nematic mixture of **13** and **RM22**; (D3) nematic mixture of **13** and **RM23**; (D4) cross-linked polymer network formed by photochemically polymerizing the nematic mixture of **13** and **RM23**.

Figure 7. Electroluminescence emission of (a) the blue-emitting component **RM23**; (b) the red-emitting component **13**; and (c) the nonpolymerized nematic mixture **13** (12%) and **RM23** (88%).
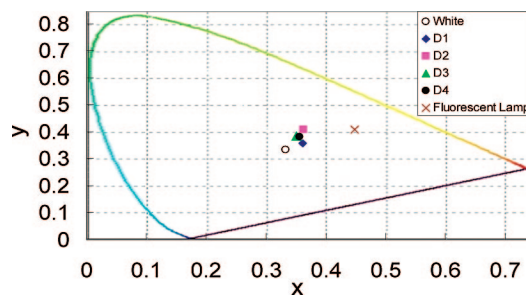
fluoride (0.6 nm) and aluminum (80 nm) were sequentially deposited in the same chamber as a combined cathode. EL was measured using a Labview-controlled Agilent E3631A DC power supply with Minolta LS100 luminance meter and Avaspec2048 fiber spectrometer.

Polarized EL. The polarized light-emitting devices were made by rubbing a PEDOT/PSS/ITO substrate. The film was first baked at 50 °C for 5 min and then at 165 °C for 10 min. The PEDOT layer was then rubbed to generate an anisotropic grooved surface in the direction of rubbing. The binary mixture of compounds **13** (12%) and **RM23** (88%) was subsequently deposited on this layer, baked at 140 °C and cooled at 5 °C/min to room temperature. The mixture was photopolymerized as discussed above. TBPi/LiF/Al layers were then deposited as above for the WOLED.

Figure 4 shows the EL spectrum of the nematic mixture of compounds **13** (12%) and **RM23** (88%) for different values of applied voltage. The emission covers most of the visible spectrum and is white. The peak EL intensity corresponds to yellow light ($\lambda_{max} = 575$ nm) with maximum sensitivity of the human eye. The shape of the EL spectrum does not change significantly with applied voltage.

Figure 5 shows the electroluminescence spectrum of the non-polymerized nematic mixture **13** (12%) and **RM23** (88%) and the corresponding EL spectrum of the cross-linked nematic polymer network formed by photochemically polymerizing this mixture. It is apparent that the differences in the spectra are slight with a small difference in the intensity of the first peak, see Figure 5.

To demonstrate the general applicability of this approach, we mixed the red-emitting LC **13** with hosts **RM21**−**RM23** in the same ratio (~1:7). The CIE coordinates (0.362, 0.358) of the nematic
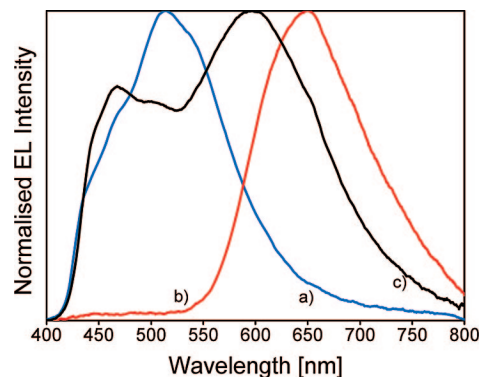
mixture **13** (12%) and **RM21** (88%) are shown in Figure 6 as point D1. The reference white point corresponds to perfect white light and the crosses represents emission from a warm, white, fluorescent light from a lamp.[3] The purity of the white-light emission from the mixture of compounds **13** (12%) and **RM22** and **RM23** (88%) is superior to that of the fluorescent light reference. White-light EL was observed for these nematic mixtures at room temperature, as shown, respectively, by the points D2 and D3 in Figure 6 corresponding to CIE coordinates (0.363, 0.407) and (0.351, 0.383). Almost no change in the CIE coordinates was observed on photochemically cross-linking the nematic mixture of the red-emitting LC **13** with the hosts **RM 23** to form an insoluble polymer network as shown by point D4. The films formed on photochemi-cally cross-linking these nematic mixtures to generate highly cross-linked polymer networks are homogeneous and no phase separation is observed, although compound **13** does not incorporate any polymerizable endgroups. Therefore, it is clear that photochemically polymerizing the nematic mixtures of the red chromophore **13** and the host nematic compound **RM23** does not affect the white light emission, although the possibility of microphase separation cannot be absolutely excluded. The shape of the EL spectrum from the cross-linked polymer network does not change significantly with applied voltage and the *x* and *y* CIE coordinates vary less than 10% between 8 and 14 V.

Figure 7 shows that the EL spectrum from the nonpolymerized nematic mixture of **13** and **RM23** is not any linear combination of the EL spectra from the individual components. Although the EL spectrum is white, the PL spectrum from the mixture is red because of Förster energy transfer from **RM23** to **13**. The intermediate EL spectrum may indicate carrier induced excimer/exciplex formation. This interesting phenomenon is under further investigation.
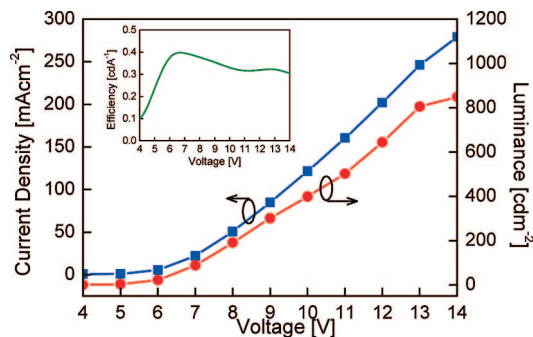
Figure 8. Luminance−voltage plot and the current density−voltage for the cross-linked nematic polymer network formed by photochemically polymerizing the nematic compounds **13** (12%) and **RM23** (88%). Inset: Device efficiency of the cross-linked nematic mixture.
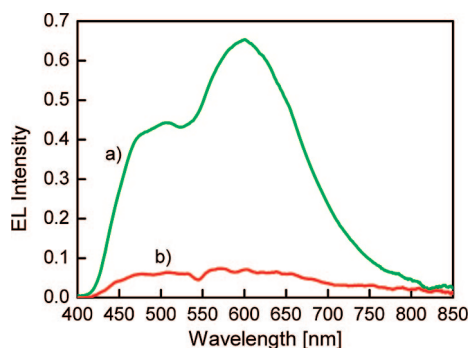
Figure 9. Polarized EL from the cross-linked nematic polymer network formed by photochemically polymerizing the nematic mixture of **13** (12%) and **RM23** (88%): (a) $EL_{||}$ and (b) $EL_{\perp}$ respectively.

Figure 8 shows the device characteristics of the white single-pixel LC-WOLED fabricated by spin-casting and photolithography of the binary mixture containing **13** and **RM23**. The LC-WOLED shows a low turn-on voltage of 4.0 V and a linear response with increasing voltage. The luminance is 190 cd m^{-2} at 8 V and 850 cd m^{-2} at 14 V. The inset shows the maximum device efficiency is 0.4 cd A^{-1}. This level of efficiency is too low for practical applications. However, it does establish a proof of principle for a new approach to white electroluminescence based on electroluminescence from liquid crystalline polymer networks. Significant improvements in performance can be realistically expected by better matching of the energy levels of device components, more efficient blue-emitting RMs, a better electron-injecting layer, and superior device fabrication procedures.[14,19]

Polarized white-light EL from the cross-linked nematic polymer network formed by photochemically polymerizing the nematic mixture of compounds **13** (12%) and **RM23** (88%) is shown in Figure 9. The alignment was achieved by mechanically rubbing the underlying PEDOT layer. A maximum polarization ratio $EL_{||}/EL_{\perp}$ of 9:1 at 600 nm is observed where $EL_{||}$ and $EL_{||}$ refer to the analyzer aligned parallel and perpendicular to the rubbing direction of the alignment layer. The $EL_{||}/EL_{\perp}$ ratio integrated over the whole spectrum is 8:1. Although these values are not very high in absolute terms they are sufficiently large to allow polarized emission with a very high polarization ratio (100:1) to be fabricated using an additional clean up polarizer. These are much cheaper than conventional polarizers and offer a cost-effective approach to WOLEDs with polarized emission. We have demonstrated a polarization ratio of 30:1 using green light-emitting liquid crystals oriented on rubbed PEDOT[37] and so significant improvements can be expected. Compound **13** should be replaced by a reactive mesogen analogue in order to eliminate any changes in orientation after cross-linking and to prevent leaching of this material from the cross-linked polymer matrix during subsequent processing. The devices reported are only bilayer WOLEDs with a PEDOT layer as the hole transport layer. A photopolymerizable electron transport/hole blocking reactive mesogen is being synthesized in order to be able to fabricate a trilayer WOLED by taking advantage of the multilayer capability of the reactive mesogen approach to WOLEDs.

Conclusion

We have mixed light-emitting liquid crystals and incorporated them as insoluble cross-linked polymer networks in an LC-WOLED that emits white light. The nature of the white-light emission is not voltage dependent and not due to Förster energy transfer. The cross-linked polymer networks can also be used to generate polarized white-light emission. This approach to WOLEDs involves deposition from solution and patterning by photolithography and potentially by inkjet printing.

(37) Woon, K. L.; Contoret, A. E. A.; Farrar, S. R.; Liedtke, A.; O'Neill, M.; Vlachos, P.; Aldred, M. P.; Kelly, S. M.; Contoret, A. E. A. *J. Soc. Inf. Display* **2006**, *14*, 557.